

# Optimization of the effects of process parameters on the tensile strength of developed aluminium roofing sheets using Taguchi method

Dickson David Olodu<sup>\*1</sup> and Andrew Eramah<sup>2</sup>

<sup>1</sup>Benson Idahosa University, Faculty of Engineering, Department of Mechanical Engineering, Benin City, Edo State, Nigeria

<sup>2</sup>Igbinedion University, Faculty of Engineering, Department of Mechanical Engineering, Edo State, Nigeria

## Article Info

### Article history:

Received 07.05.2023

Revised: 14.06.2023

Accepted: 30.06.2023

Published Online: 30.09.2023

### Keywords:

Aluminum roofing sheets

Design of experiments

Orthogonal array

S/N ratio

Taguchi method

## Abstract

This study employed the Taguchi Method to optimize the impact of process factors on the tensile strength of newly designed aluminum roofing sheets. The Taguchi Method which is a statistical approach was utilized to improve the manufacturing quality of aluminum roofing sheets. The performance characteristics of process factors on the tensile strength of the generated aluminium roofing sheets were investigated using an orthogonal array, a signal-to-noise ratio, and an analysis of variance. Four variables such as production temperature, production pressure, cooling time, and the percentage of chromium in the aluminum roofing sheet were taken into account in this analysis. An appropriate orthogonal array was chosen, and tests were run. The process parameters were assessed following the experimentation, and the signal-to-noise ratio (S/N ratio) was computed. The best parameter values were found with the use of graphs, and confirmation trials were run to ascertain the adequacy of the tensile strength of the aluminum roofing sheets produced. The outcome demonstrated that a production temperature of 1610°C, a production pressure of 79 GPa, a cooling time of 85 seconds, and a chromium content of 2.0% gave an aluminum roofing sheet its optimum tensile strength of 592 MPa. The manufacturing temperature, followed by cooling time and the percentage of chromium, was shown to have the most significant impact on the tensile strength of aluminum roofing sheets. The least effective component was determined to be production pressure. Moreover, the metallographic examination of the grain refined aluminum alloy showed a lower level of porosity defect and higher tensile strength compared with the unrefined alloy (pure aluminum). Also, the refined alloy shows lower aquiaxed structure compared with the unrefined alloy (pure aluminum).

## 1. Introduction

The microstructure of commercial-pure aluminum (LXX Series), which contains more than 99% aluminium is mostly made up of pure aluminum FCC matrix. The non-metallic inclusions, which are caused by the presence of iron and silicon impurities, are the other current phases. Unalloyed aluminum can be strengthened by cold working but cannot be heat treated. Due to the face-centered cubic (FCC) crystal structure of aluminum and its alloys, they have outstanding formability characteristics, with the exception of the restriction caused by the level and kind of alloying. Some aluminum alloys can be heat-treated to a greater degree of strength than many structural steels [1]. The metal possesses a pleasing surface finish, good thermal and electrical conductivity, good reflectivity, and low density [1, 2]. These alloys are the main structural materials in the aircraft industry as a result of this last characteristic, which, when combined with the high strengths available, results in high strength-to-weight ratios. Aluminum's stiffness (elastic modulus) is only roughly one-third that of steel; therefore, this fact must be taken into account when designing components to avoid excessively significant deflections in use [3-5].

Moreover, grain refinement is the act of controlling the solidification process to produce more (and subsequently smaller) grains as well as grains of a particular shape. The

phrase "refinement" typically refers to the addition of chemicals to the metal, but it can also refer to the regulation of cooling speed. Any substance added to a liquid metal to produce a finer grain size in the ensuing casting is known as a grain refiner [6]. AL-6Ti, AL-5Ti-1 B, and AL-5Ti-1C are the master alloy additions for aluminum alloys that are most readily available [7]. The composition of the alloy, the pace of solidification, and the addition of grain refiners containing intermetallic phase particles serves as sites for heterogeneous grain nucleation which affect the type and size of grains that are produced. In order to increase casting soundness, a finer grain size reduces shrinkage, hot cracking, and hydrogen porosity. The feeding qualities, mechanical properties, thermal treatment response, pressure tightness, appearance after chemical, Electro-chemical, mechanical finishing, and higher wear resistance were all improved by grain refinement [8, 9, 10]. Adding particles to the melt that form new crystals during solidification is the most effective way to adjust grain size. In addition, the kind and weight percentage of grain refining additives have an impact on the grain size and tensile strength of aluminum alloys. TiB<sub>2</sub>, Fe, and Cr can be used for refinement of aluminium.

Aluminum and composite materials are widely employed in a variety of industry sectors, including aerospace, automotive, and marine. Due to their frequent use,

experimental research is needed to develop these materials' strength and repair capabilities [11]. These materials need to be created through expensive and time-consuming experimental research. As a result, interest in numerical analysis has increased [11]. The main draw of numerical analysis is how closely it resembles experimental findings [11]. A statistical approach called the Taguchi method was developed by Taguchi and Konishi [12]. Initially, it was established to improve the quality of manufactured items (development of production processes), but later its application was extended to many other engineering disciplines, such as biotechnology [13]. The invention of the analysis of variance method was one of Taguchi's achievements that was particularly valued by statisticians in the field. To successfully obtain the desired outcomes, precise process parameter selection and their separation into control and noise components are essential [12, 14]. In this design of experiment, the control is selected in such a way as to eliminate the influence of the sound source in order to achieve the best process results. Taguchi's method involves determining the appropriate control parameters which entails that a number of orthogonal network (OA) tests is performed [15]. Data analysis and component quality prediction methods use the results of these studies [16]. Foster [7] looked into how five input characteristics affected the refined goods' surface quality. The input parameters were mold temperature, melting temperature, packing pressure, packing duration and injection time. To reduce the shrinkage of polypropylene (PP) and polystyrene (PS), the Taguchi process was used. In addition, he also used neural networks to simulate the process and reduced PP and PS by 0.937% and 1.224% respectively. Vaatanen et al. [18, 19] used the Taguchi method to analyze the effect of injection molding parameters on the aesthetic quality of cast parts; weight, welding, and kiln marks were three other quality attributes targeted for reduction. With very little experience, they are able to optimize various quality features that can lead to cost savings.

The discovery of new materials through research and design is the driving force behind economic development [20]. That is, modern technology is highly dependent on material research, which contributes to the progress of the economy of each country. Kok [21] studied the mechanical properties of vortex produced composites of 2024 aluminum alloy enriched with  $Al_2O_3$  particles. The hardness and toughness of MMC A359/ $Al_2O_3$  increased with rising temperature, according to Kumar et al. [22]. In addition, their research showed that the use of electromagnetic agitation during production leads to smaller particles and better adhesion from the interface of the particles to the matrix. Al/SiC composites produced by powder metallurgy were studied by Venkatesh and Harish [23] to obtain the required properties and improve the mechanical properties of aluminum. Nie and Chelman [24] and Friends [25] reported that aluminum strength, fatigue strength, modulus, wear resistance and creep are improved by reinforcement. Yao et al., [26] reported the study of aluminum trimodal metal matrix and the parameters affecting their strength; Tensile strength, which is significant in many applications, is the most useful and commonly referenced assessment of these characteristics [26]. For composites reinforced with  $TiB_2$  particles, Saravanan et al. [27] found a 30% increase in stiffness and almost a doubling of tensile strength compared to the base aluminum alloy. The impact of mixing duration and speed on particle dispersion in SiCAMC

was studied by Prabu et al. [28]. Nie et al. [24] reported that the aluminum material's strength, durability, and stability all declined. Early processing observations showed that porosity and an unequal distribution of reinforcement in the form of groups or clusters of reinforcement persisted [24]. Additionally, for a particular matrix alloy, decreasing the volume fraction reduces the break duration [20, 22]. Joardar et al. [29] analysed the deformation behavior of solid aluminum matrix cylinders under dry conditions. According to Romanova et al. [30], technical parameters such as the aspect ratio (ratio of height and diameter) of the specimens and the test temperature have a significant effect on the compressive strength and performance of aluminum. According to Domnita et al.'s [31] investigation into the effects of reinforcing particle shape and interface strength on the deformation and fracture behavior of an Al/ $Al_2O_3$  composite, two pathways for particle failure are cracking and separation at the interface. Adin and şcan [32, 33] used the Taguchi approach to optimize the process parameters of medium-carbon steel joints connected by MIG welding. According to their findings, groove angle was shown to be the characteristic that had the greatest impact on both average tensile strength and elongation. For a particular 6061-T6 Al alloy, Yildiz [34] investigates the relationships between the Charpy V-notch test and fracture toughness. To ascertain the deformation behavior of the investigated alloys, tensile tests were used. Additionally, Charpy V-notch experiments were conducted to measure absorbed energy under mild impact conditions; the results of these tests are consistent with prior literature. A numerical analysis of the fatigue behavior of unpatched and patched aluminum and composite plates is conducted by Hamit et al. [11]. They used mathematics to investigate the fatigue behavior of composite patched and unpatched Al 5083 aluminum plates. The numerical research used the Finite Element Method. The Ansys version 15.0 Workbench Package application was used to perform numerical analyses for this work. The "V" notched and patched specimens with a 30° angle show the highest fatigue life (1593.2 N), respectively.

The goal of this study was to employ the Taguchi Method to optimize the impacts of process factors on the tensile strength of newly created aluminum roofing sheets. Before choosing this aluminum alloy, the 5052 aluminum alloy's durability and adaptability in applications were taken into account.

## 2. Materials and methods

### 2.1 Materials

The strongest non-heat-treated sheet and plate in widespread use, aluminum 5052 alloy sheet, was used in this study. It is one of the most useful alloys due to its versatility and excellent value. The Differential Aluminum Company in Benin City, Edo State, Nigeria, provided the aluminum 5052 sheet. In order to regulate the grain structure, limit grain growth, and avoid recrystallization following heat treatment in aluminum roofing sheets or aluminum-magnesium-zinc alloys, chromium (Cr) was added at different percentage to the aluminum. The percentage of Cr ratios used in this study were chosen and ranges from 0.5% to 3.0% respectively. The Chromium added was used to improve toughness and reduces susceptibility to stress corrosion. After cooling, the mechanical properties of these materials, which were created at different pressures and temperatures were evaluated. This material was exposed to a range of pressures and temperatures ranges from

40 GPa to 82 GPa and 670°C to 2400°C respectively during production.

Additionally, a 5025 aluminum alloy including chromium had its tensile strength evaluated. X-ray microanalysis and energy dispersive spectroscopy were used to evaluate the microstructure. The investigated specimens displayed complex phases based on the addition chromium. It was discovered that alloys with a larger quantity of chromium had fewer precipitation-hardening effects.

### 2.2. Measurement of temperature and pressure

A stationary non-contact infrared pyrometer was used to measure the temperature of aluminum alloys during the manufacturing process. This instrument has higher measurement accuracy than other temperature measuring instruments. It is applied in machine maintenance, process control and quality control. Infrared pyrometers can accurately measure in hazardous and hard-to-reach areas that could pose a danger to workers. Infrared pyrometers with sensitivity of 88.7% (within  $\pm 0.3$  °C) can measure temperatures above 2500°C. In addition, a pressure sensor was also used to measure the pressure of the molten aluminum alloy during production. The equipment is integrated into the aluminum production plant.

### 2.3. Data collection method

Various samples of designed aluminum roofing sheets manufactured at different temperatures and pressures were tested with strain gauge testing machines according to the requirements of the Tensile test specimens for the American Society for Testing and Materials (ASTM) were made to the required design length. Tensile standard specimens according to ASTM E8-09 were ready for testing. The mean values were calculated after testing a total of thirty-six (36) samples. Before the tensile test, the ASTM E8M-compliant samples were thoroughly cleaned once again to remove any remaining contaminants like rust, oil, and dirt. A 250 kN Shimadzu universal tester was used to conduct tensile testing at room temperature, 50–5% humidity, and 2 mm/min crosshead speed [11]. Figure 3 depicts the experimental study's tensile testing apparatus. The stock was cut into three separate discarded test pieces, each measuring 45 mm in gauge length and 9 mm in diameter. Figure 1 illustrates the tensile specimens' dimensions. The universal lathe machine was used to machine the tensile test specimens to the necessary specifications.

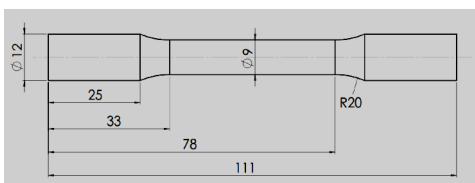


**Figure 1.** The dimensions of the tensile testing specimen in relation to ASTM E8-09 [1]

### 2.4. Evaluation of engineered aluminum roof sheets for tensile strength

The aluminum roofing sheet samples developed were evaluated for their mechanical strength (tensile strength) according to Equation 1 [14].

$$\text{Tensile Strength} = \frac{\text{Maximum Load}}{\text{Original Cross-Sectional Area}} \quad (1)$$

### 2.5. Preparation of specimens for metallographic investigation

In this investigation, samples of aluminum with and without a grain refiner (addition of Chromium) were prepared in a way that virtually eliminates all flaws. For metallographic and mechanical tests, specimens of pure aluminum and aluminum with refinements were developed. The length of the samples used for metallographic analysis is 15 mm. For metallographic analysis, specimens of pure aluminum and aluminum with Chromium were produced to analyze the structural configuration. For tensile strength tests, specimens with and without grain refinement were produced. Homogenization was used to treat the Al-pure, and the T4 technique was used to anneal the refined specimens.



**Figure 2.** The tensile test specimen

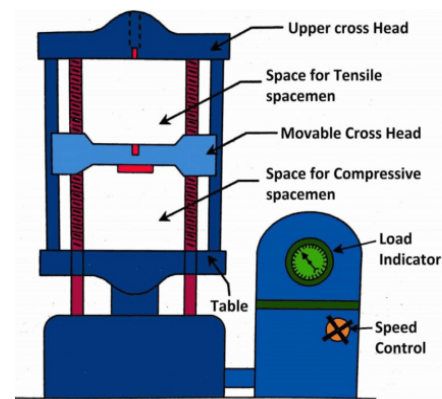


**Figure 3.** Universal testing machine

### 2.6 Metallographic investigation

The aluminum samples were examined and photographed. The samples were cleaned in water and alcohol before being dried in a warm air stream. All of the metallographic studies conducted for this study employed a Nikon AFX-11 optical microscope equipped with a 35mm camera. To see the grain, all samples with or without grain refinement were examined under the Nikon AFX-11 optical microscope.

### 2.7. Optimization of aluminium roofing sheets process parameters using Taguchi method

#### 2.7.1. Experimental plan

This is one of the most thorough methods for developing a product or process is experimental design. Through a number of experiments, this statistical approach seeks to provide predictive knowledge about a challenging, multivariate process. The main design of experiments (DOE) strategy is as follows:

#### 2.7.2. Taguchi method

A full factorial design necessitates a great deal of testing. As the number of parameters rises, this takes more time and becomes more complicated. Taguchi developed an innovative method employing an orthogonal array to explore the whole parameter space with fewer experiments to address this issue. In order to measure performance that deviates from the ideal target value, Taguchi advises employing a loss function [12].

A signal-to-noise (S/N) ratio is then created from the value of this loss function. The Taguchi method uses a signal-to-noise (S/N) ratio that reflects both the mean and variability of quality characteristics. It is a metric of effectiveness for creating systems and procedures that are resistant to noise influences.

2.8. Types of S/N Ratio

(i) *Smaller-the-better*: In Smaller-the-better,

$$\text{Signal to noise ratio, } \eta \left( \frac{S}{N} \right) = -10 \text{Log}_{10} \left\{ \frac{1}{n} \sum_{i=1}^n y_i^2 \right\} \quad (2)$$

When a characteristic's minimization is desired, it is utilized.

(ii) *Larger-the-better*: In Larger-the-better

$$\text{Signal to noise ratio, } \eta \left( \frac{S}{N} \right) = -10 \text{Log}_{10} \left\{ \frac{1}{n} \sum_{i=1}^n \frac{1}{y_i^2} \right\} \quad (3)$$

Where i ranges from 1 to n, and n is the number of iterations used to complete tasks that call for optimizing the quality traits of interest with S/N (signal-to-noise ratio), n (number of observations), and yi (i-th number of observations).

(iii) *Nominal-the-best*: Equation 4 is used to determine the signal ratio for Norminal-the-best:

$$\text{Nominal - the - best } \left( \frac{S}{N} \right) = -10 \text{Log}_{10} \left\{ \frac{\mu^2}{\sigma^2} \right\} \quad (4)$$

when the mean,  $\mu$  and standard deviation,  $\sigma$  are given. It is applied while attempting to reduce the RMS error near a particular target value. Matching the mean to the objective transforms the issue into a constrained optimization problem, regardless of the approach.

2.8.1. Selected signal ratio

In this study, the smaller-the-better was used. This is because production temperature ( $^{\circ}\text{C}$ ), production pressure

(GPa), cooling time (second) and percentage of chromium in aluminium roofing sheet (%) are intended to be lower in order to produce aluminium roofing sheets with good tensile strength.

2.9. Identifying the control factors and their levels

L9 orthogonal array and three processing parameter levels were chosen. Table 1 displays the process parameters and levels, while Table 2 displays the L9 orthogonal array.

3. Results and discussion

3.1. Microstructure examination of pure aluminum and aluminum with chromium (cr)

Figure 4a to 4e shows the microstructures of pure aluminum and aluminum alloys with different additives of (Cr) percentages.

3.2. Discussion of microstructure pure aluminium and aluminium with different additives of chromium (Cr)

3.2.1 Metallographic investigation

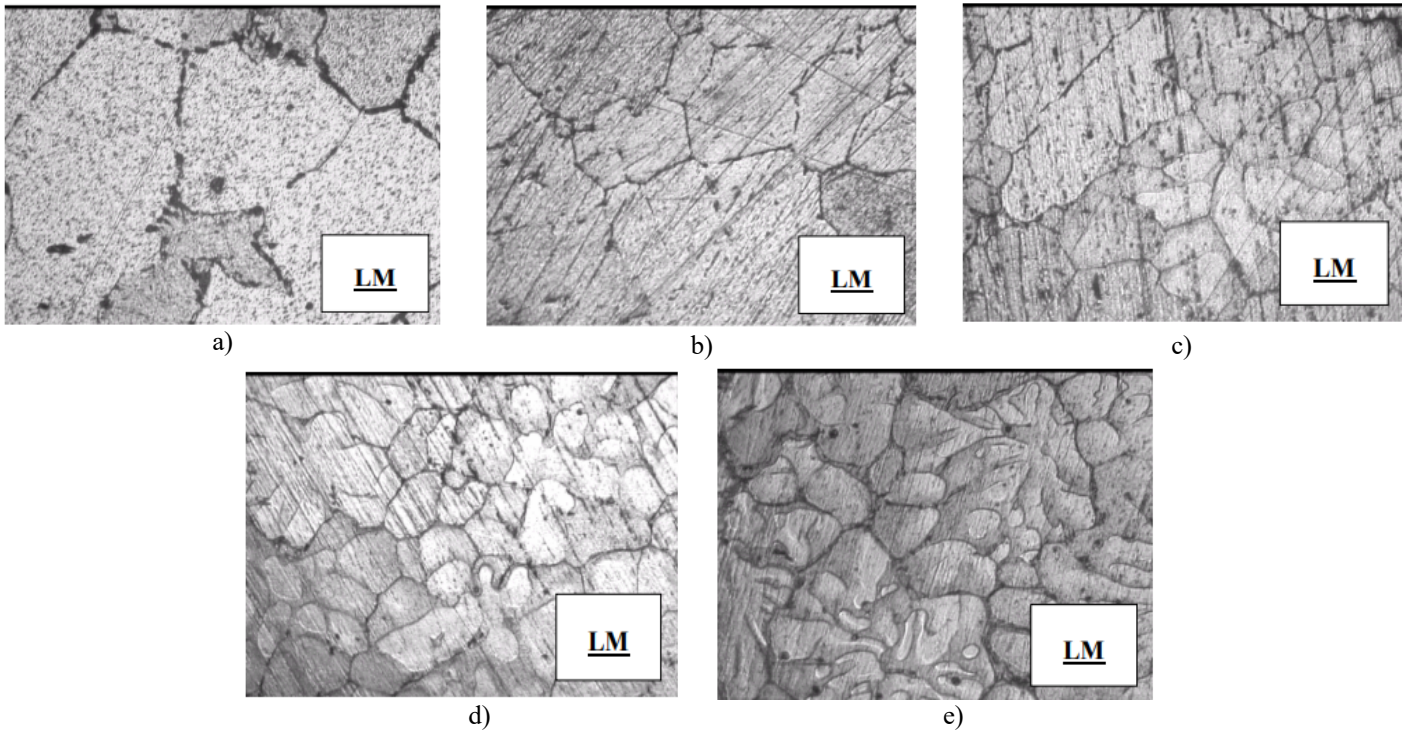
Compared to the unprocessed alloy (pure aluminum), the grain-refined alloys had a lower level of porosity defects, according to metallographic analysis. Additionally, as illustrated in Figure 4, the refined alloy has a less aquiaxed structure than the unprocessed alloy (pure aluminum). A finer grain was produced when grain refinement was added to the examined alloy. For the addition of 2.0% Cr, the addition of a grain refiner provides effective refining. Moreover, less refinement was obtained by the other percentages of chromium refiners. Figures 4a to 4e demonstrate that there is a somewhat notable difference between the crude and polished structure. This may be due to the fact that the initial raw material (commercial pure aluminum) contains several impurities like Ti, Zn, and B that serve as advantageous sites for nucleation when oxygen or sulfur are included.

Table 1. The process parameters and their levels

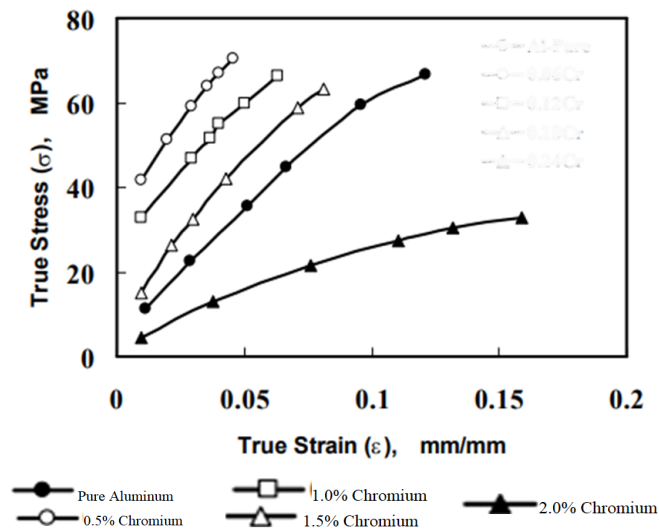
Serial Number	Factors	Level 1	Level 2	Level 3
1	Production Temperature ( $^{\circ}\text{C}$ )	1022	1610	2001
2	Production Pressure (GPa)	40	65	79
3	Cooling Time (second)	44	60	85
4	Percentage of Chromium in Aluminium Sheet (%)	0.5	2.0	3.0

Table 2. The orthogonal array for L9

Experiment Number	Control Factors			
	Production Temperature ( $^{\circ}\text{C}$ )	Production Pressure (GPa)	Cooling Time (second)	Percentage of Chromium in Aluminium Sheet (%)
1	1	1	1	1
2	1	2	2	2
3	1	3	3	3
4	2	1	2	3
5	2	2	3	1
6	2	3	1	2
7	3	1	3	2
8	3	2	1	3
9	3	3	2	1



**Figure 4.** Microstructures of samples; a) pure aluminum, b) Al ± 0.5% Cr, c) Al ± 1.0% Cr, d) Al ± 1.5% Cr and e) Al ± 2.0% Cr



**Figure 5.** Pure aluminium (Al-Pure) with different Additives of chromium

**3.2.2 Effect of Grain Refining Additions**

The casting process was used to study the effects of grain refining additives, such as Cr, on increasing the mechanical characteristics and grain refining of pure aluminum. Optical microscopy was used to examine the effects of grain refining during the material production process following casting. Tensile strength tests and experimental findings for aluminum produced with and without additions of grain refiner were investigated. It was observed that the presence of Cr as a master alloy affect the tensile strength of the various refinements of aluminum.

**3.2.3. Grain Refining Effect on the Flow Stress**

When compared to the ductility of pure aluminum (Al-pure), the tensile behavior of all refined specimens shows high ductility. According to Figure 5, all of the tensile specimens with various additive addition percentages exhibit an increase in flow stress when compared to pure aluminum. Except for the specimens with 2.0% Cr, which recorded the lowest flow stress as shown in Figure 5. The effect of grain refining with various grain refining additives is noticeable in general. Figure 5 illustrates how the flow stress value for the alloy with the addition of 0.5% Cr is greater than that for pure aluminum by roughly 50% and greater than that for all other additions combined.

**3.3. Optimization results using Taguchi method**

The components and levels listed in Table 1 were used in the studies, per the orthogonal table (OA) above. Table 3 presents the experimental configuration with the chosen factor values. Each of the nine aforementioned experiments was carried out. 36 trials were conducted a total of four times to account for potential changes brought on by noise sources. The measured values of the process parameters acquired from various tests are displayed in Tables 4 through 7.

**3.1 Determining the Experimental Matrix**

The orthogonal table (OA) above indicates that the components and levels used in the trials were those listed in Table 1. Table 3 displays the experimental configuration with the chosen values for the factors. Each of the nine aforementioned experiments was carried out. Four (4) times (that is, a total of 36 experiments) to account for potential changes brought on by noise elements. The measured values of the process parameters derived from several tests are displayed in Tables 4 to 7.

**Table 3.** Orthogonal array with control factors and tensile strength for aluminium roofing sheets

Experiment Number	Control Factors				Tensile Strength (MPa)
	Production Temperature (°C)	Production Pressure (GPa)	Cooling Time (second)	Percentage of Chromium in Aluminium Sheet (%)	
1	1022	40	44	0.5	342
2	1022	65	60	2.0	469
3	1022	79	85	3.0	543
4	1610	40	60	3.0	452
5	1610	65	85	0.5	600
6	1610	79	44	2.0	621
7	2001	40	85	2.0	612
8	2001	65	44	3.0	602
9	2001	79	60	0.5	594

**Table 4.** Measured values of production temperature for aluminium roofing sheets

Experiment Number	Production Temperature (°C)				
	1	2	3	4	Mean
1	1023	1020	1025	1020	1021.50
2	1190	1200	1198	1196	1196.00
3	1372	1442	1432	1439	1421.25
4	1600	1610	1601	1596	1601.75
5	1792	1800	1788	1790	1792.50
6	1921	1921	1920	1930	1923.00
7	1991	2001	1990	1985	1991.75
8	1023	1024	1034	1030	1027.75
9	1189	1200	1190	1196	1193.75

**Table 6.** Measured values of cooling time for aluminium roofing sheet production

Experiment Number	Cooling Time (second)				
	1	2	3	4	Mean
1	41	42	44	43	42.50
2	45	44	47	48	46.00
3	48	54	51	50	50.75
4	56	58	57	59	57.50
5	58	62	58	61	59.75
6	60	65	66	63	63.50
7	72	73	74	71	72.50
8	74	76	77	75	75.50
9	81	80	82	85	82.00

**Table 5.** Measured values of production pressure for aluminium roofing sheets

Experiment Number	Production Pressure (GPa)				
	1	2	3	4	Mean
1	38	43	40	42	40.75
2	54	53	56	56	54.75
3	61	60	62	62	61.25
4	66	68	65	63	65.50
5	69	68	69.5	70	69.125
6	72	71	72	73	72.00
7	73	75	74	76	74.50
8	76.5	77	76	78	76.875
9	80	77	78	79	78.50

**Table 7.** Measured values of percentage of chromium in aluminium roofing sheets (%)

Experiment Number.	Percentage of Chromium in Aluminium Roofing Sheet (%)				
	1	2	3	4	Mean
1	3.0	0.5	3.0	2.0	2.125
2	0.5	1.2	1.3	1.2	1.050
3	0.8	2.0	0.8	2.3	1.475
4	1.0	1.6	1.0	0.8	1.100
5	2.0	2.2	2.0	0.6	1.700
6	1.5	3.0	1.5	0.5	1.625
7	2.5	2.1	2.5	2.3	2.400
8	1.8	1.7	1.8	2.8	2.025
9	1.2	1.2	1.2	1.9	1.375

**Table 8.** Tabulated signal-to-noise ratios for of aluminium roofing sheets

Experiment Number	S/N Ratio (dB) for Production Temperature (°C)	S/N Ratio (dB) for Pressure (GPa)	S/N Ratio (dB) for Cooling Time	S/N Ratio (dB) for Percentage of Chromium in Aluminium Sheet (%)
1	-60.1890	-32.2122	-32.5708	-7.4527
2	-61.5550	-34.7701	-32.1445	-0.8099
3	-63.0550	-35.7429	-34.1166	-4.2202
4	-64.0919	-36.3281	-35.1950	-11.3943
5	-65.0692	-36.7932	-35.5306	-5.1851
6	-65.6796	-37.1471	-36.0611	-5.3624
7	-65.9847	-36.2185	-37.2078	-7.4429
8	-60.2378	-36.4741	-37.5599	-6.3372
9	-61.5383	-37.8982	-38.2785	-2.9721

For each of the different control parameters, the S/N ratio ( $\eta$ ) is determined as shown below:

Sum of Squares for production temperature from 1 to 3;

$$S_{T1}=(\eta_1+\eta_2+\eta_3) \tag{5}$$

Sum of Squares for production temperature from 4 to 6;

$$S_{T2}=(\eta_4+\eta_5+\eta_6) \tag{6}$$

Sum of Squares for production temperature from 7 to 9;

$$S_{T3}=(\eta_7+\eta_8+\eta_9) \tag{7}$$

Sum of Squares for production pressure from 1 to 3;

$$S_{P1}=(\eta_1+\eta_4+\eta_7) \tag{8}$$

Sum of Squares for production pressure from 4 to 6;

$$S_{P2}=(\eta_2+\eta_5+\eta_8) \tag{9}$$

Sum of Squares for production pressure from 7 to 9;

$$S_{P3}=(\eta_3+\eta_6+\eta_9) \tag{10}$$

Sum of Squares for cooling time from 1 to 3;

$$S_{T1}=(\eta_1+\eta_5+\eta_9), \tag{11}$$

Sum of Squares for cooling time from 4 to 6;

$$S_{T2}=(\eta_2+\eta_6+\eta_7) \tag{12}$$

Sum of Squares for cooling time from 7 to 9;

$$S_{T3}=(\eta_3+\eta_4+\eta_8) \tag{13}$$

Sum of Squares for percentage of chromium from 1 to 3;

$$S_{C1}=(\eta_1+\eta_4+\eta_7) \tag{14}$$

Sum of Squares for percentage of chromium from 4 to 6;

$$S_{C1}=(\eta_2+\eta_5+\eta_8) \tag{15}$$

Sum of Squares for percentage of chromium from 7 to 9;

$$S_{C1}=(\eta_3+\eta_6+\eta_9) \tag{16}$$

See Table 9 to choose values for  $\eta_1, \eta_2, \eta_3$ , etc., and to calculate  $S_1, S_2$ , and  $S_3$ . The S/N ratio for this experiment,  $\eta_{jk}$ , is denoted by the symbol  $k$ . For level 1 production temperatures, the typical S/N ratio is  $\frac{ST_1}{3}$ . For level 2 production temperatures, the typical S/N ratio is  $\frac{ST_2}{3}$ . The typical S/N ratio for level 3 production temperatures is  $\frac{ST_3}{3}$ .

Every factor's comparable level is  $j$ . The production pressure, cooling time, and chromium content of aluminium roofing sheets are each calculated using comparable formulae. The average signal-to-noise ratio is shown in Table 9.

**Table 9.** The response table for s/n ratio for aluminium process parameters

Serial Number	Production Temperature (°C)	Production Pressure (GPa)	Cooling Time	Percentage of Chromium in Aluminium Sheet (%)
Level 1	-61.5997	-34.2417	-32.9440	-4.1609
Level 2	-64.9469	-36.7561	-35.5956	-7.3139
Level 3	-62.5869	-36.8636	-37.6821	-5.5841
DELTA	3.3472	2.6219	4.7381	3.1530
RANK	2	4	1	3

\*DELTA= Absolute highest signal Noise ratio - Absolute Lowest signal Noise ratio

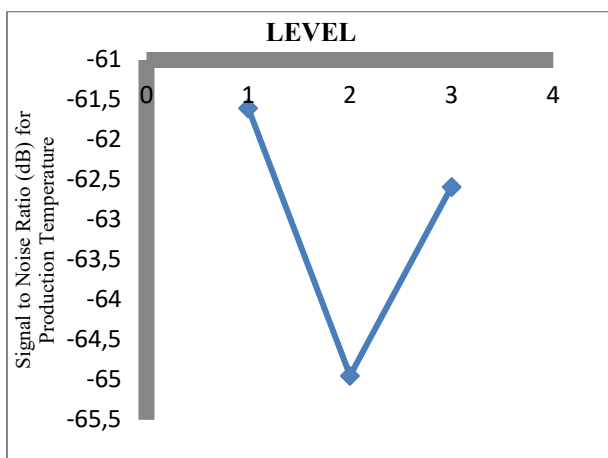


**Figure 6.** Signal to noise ratio for production temperature

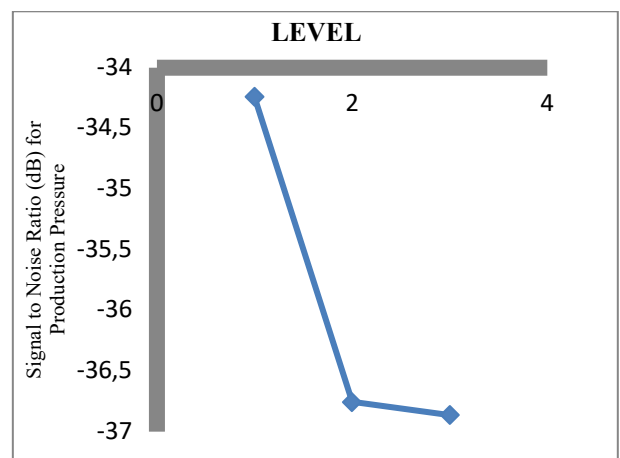


**Figure 7.** Signal to noise ratio for production pressure

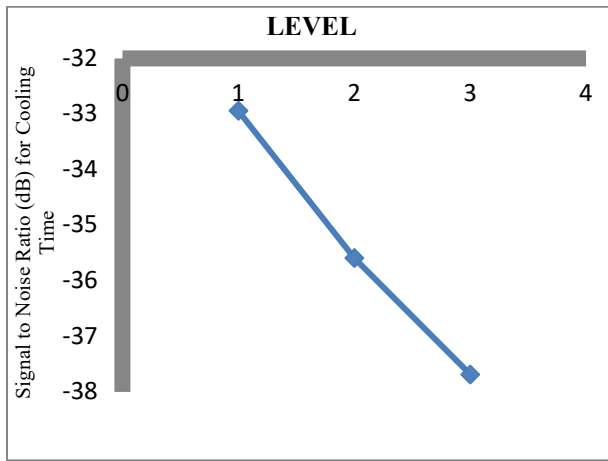


Figure 8. Signal to noise ratio for cooling time

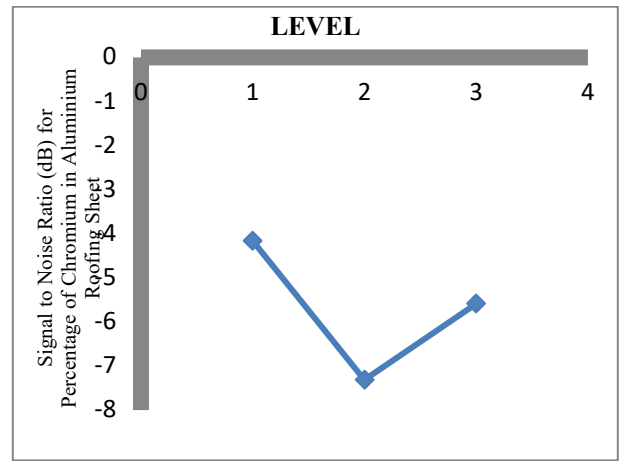


Figure 9. Signal to noise ratio for percentage of chromium in aluminium roofing sheet (%)

3.2. Confirmation experiment

The confirmation experiment, which was performed using manufacturing parameters of 1610 °C, 79 MPa, 85 s of cooling time, and 2.0% chromium in aluminum roofing sheets, is shown in Table 11. A total of five sets of experiments were run in the confirmation experiment, and their tensile strength was assessed. It is evident that the outcomes were reliable.

Table 10. Optimum values of factors of developed aluminium roofing sheets

Process Parameter	Optimum Value
Production Temperature (°C)	1610°C
Production Pressure (MPa)	79 GPa
Cooling Time (second)	85 seconds
Percentage of Chromium in Aluminium Roofing Sheets (%)	2.0%

Table 11.: Confirmation experiment

Process Parameters					
Serial Number	Production Temperature (°C)	Production Pressure (MPa)	Cooling Time (second)	Percentage of Chromium in Aluminium Roofing Sheets (%)	Tensile Strength (Mpa)
1	1610	79	85	2.0	592.0
2	1610	79	85	2.0	592.5
3	1610	79	85	2.0	591.5
4	1610	79	85	2.0	591.0
5	1610	79	85	2.0	593.0
Mean Tensile Strength					592

3.3 Discussion of Results from Optimization using Taguchi method

The response table for the S/N ratio is shown in Table 9. The best set of combination parameters was determined to be the one with the highest value for each factor. The ideal process parameter combinations for aluminum roofing sheets are LEVEL 2 for production temperature, LEVEL 3 for production pressure, LEVEL 3 for cooling time, and LEVEL 2 for chromium content. The delta value in Table 9 illustrates the variable that has the largest influence on the tensile strength of aluminum roofing sheets. The factor with the biggest effect on the tensile strength of aluminum roofing sheets was found to have a delta value for cooling time of 4.7381. Production temperature, with a Delta value of 3.3472, production pressure, with a Delta value of 2.6219, and the percentage of chromium all came after that (Table 9). A response diagram for the generated S/N ratio is shown in Figure 6-9. The greatest S/N ratio for each factor was used to calculate the optimal process condition, which corresponds to a production temperature of 1610 °C, a production pressure of 79 GPa, a cooling time of 85 seconds, and a chromium percentage of 2.0% (Table 10). The

factor levels with the highest S/N ratio were chosen to help the problem. The confirmation experiment further demonstrates that a mean tensile strength of 592.0 MPa was achieved. The mechanical characteristics of vortex-produced composites of 2024 aluminum alloy enhanced with Al<sub>2</sub>O<sub>3</sub> particles were investigated by Kok [21]. For the production process, 700°C for casting, 550°C for mold preheating, 900 rpm for mixing speed, and 5 g/min for particle addition speed are the ideal melting temperatures, mold preheating temperatures, mixing speeds, particle addition speeds, mixing times, and contact pressure. The mixing period is 105 seconds, and the contact pressure is 6 MPa. The obtained production temperature is consistent with this investigation. Adin and Şcan [32] used the Taguchi approach to optimize the process parameters of medium-carbon steel joints connected by MIG welding. The results revealed that the groove angle of 90°, the current of 120 A, and the voltage of 30 V produced the greatest tensile strength of 597.963 MPa and the lowest tensile strength of 395.125 MPa. The optimal tensile strength value of 592 MPa found in this investigation agrees with the highest tensile strength of 597.963 MPa. A numerical analysis of the fatigue



behavior of unpatched and patched aluminum and composite plates is conducted by Hamit et al. [11]. They used mathematics to investigate the fatigue behavior of composite patched and unpatched Al 5083 aluminum plates. The toughness results obtained in their study serves as a basis for the tensile strength obtained in this study. The obtained values in this study were used to improve the material property (tensile strength) of aluminum roofing sheet in aluminum production industries.

#### 4. Conclusion

Chromium (Cr) additives in varying concentrations, ranging from 0.5% Cr to 2.0% Cr was added to pure aluminium. It was used to refine grains of commercially pure aluminum. The grain size reduces as the percentage of additives increases. As the ratio of chrome grows in Cr additions, so does the refined alloy's tensile strength increases. The best combinations of manufacturing conditions for the tensile strength of aluminum roofing sheets were found using the Taguchi method. According to the results, the optimum mean tensile strength of 592Mpa was obtained at manufacturing temperatures of 1610 °C, production pressure of 79 GPa, cooling time of 85 seconds and percentage of chromium of 2.0%. The most important aspect was discovered to be cooling time, which was followed by manufacturing temperature and chromium content. The least effective component was determined to be production pressure. This study is intended to help researchers and manufacturers of aluminum develop high-quality, defect-free aluminum roofing sheets, which would ultimately boost productivity in the aluminum industries.

#### Author Contributions

The percentages of author(s) contributions are presented below. All authors reviewed and approved final version of the manuscript.

%	D.D.O.	A.E
C	60	40
D	60	40
S	50	50
DCP	50	50
DAI	60	40
L	50	50
W	50	50
CR	60	40
SR	60	40
PM	50	50
FA	50	50

C= concept, D= design, S= supervision, DCP= data collection and/or processing, DAI= data analysis and/or interpretation, L= literature search, W= writing, CR= critical review, SR= submission and revision, PM= project management, FA= funding acquisition.

#### Conflict of Interest

In this project, there was no conflict of interest in the review, collection of data, analysis of data, in the writing of the manuscript, or in the decision to publish the results.

#### Acknowledgments

The authors acknowledged the Department of Mechanical Engineering, Faculty of Engineering, Benson Idahosa University and Igbinedion University respectively for the using some of their facilities during the fabrication process.

#### References

- Elmas, S., Ageing behaviour of Spray Coat Al-Zn-Mg-Cu Alloys, *Turk journal of Engineering Environmental Science*, **2022**, 25: 681-686
- Song, W., The Effect of Thermal Ageing on the Alorasive Wear Behavior of Age Hardening Al/Sic and 6061 Al/Sic Composite. *Wear Journal*, **2023**, 185: 125-130
- Lee, W., The Strain Rate and Temperature Dependence of the Dynamic Impact Properties of 7075 Aluminum Alloy, *Journal of Materials Processing Technology*, **2020**, 100: 116-122
- Kagawa, Y., Temperature Dependence of Tensile Mechanical Properties in SiC Fiber Reinforced Ti Matrix composite, *Journal of Engineering*, **1994**, 2 (9): 3019-3026
- Jingyu, L., Tingqi, Q., Zhanli, C., Wanze, Z., Minglong W., Chuanzhi Du., Study of vibration frequency-fatigue strength action of 6061-T6 aluminum alloy during fillet welding, *Journal of Vibroengineering*, **2021**, 8: 1-16
- El-Nasser, G.A., Nassef, A.E., and El-Soeudy, R.I., Modification of AA7075 Alloy by Addition of Al-5Ti-1B Alloy, 5th International Engineering Conference, **2006**, 27-3
- Sofyan, B., Abseptions of the Effect of Zn on Precipitation Processes in an Al-Cu-Mg-Ag Base Alloy, *Journa of Material Science*, **2020**, 337: 977-982
- Yoshimi, W., Noboru, Y., Yasuyoshi, F., Wear Behaviour of Al-Al<sub>3</sub>Ti Composite Manufactured by a Centrifugal Method, *Metallurgical and Materials Transactions A*, **1999**, 30: 3253-3261
- Lee, K., Fabrication of Al-3Wt PCT Mg Matrix Composites Reinforced with Al<sub>2</sub>O<sub>3</sub> and SiC Particulates by the Pressureless Infiltration Technique, *Metallurgical and Materials Transactions*, 1998, 29: 3087-3094
- Song, N., Shi, G.T., Gray III & Roberts, J. A., Reinforcement Shape Effect on the Fracture Behavior and Ductility of Particulate Reinforced 6061Al Matrix composite, *Metallurgical and Materials Transactions A*, **1996**, 27:3739-3355
- Hamit, A., Sağlam, Z., & Adin, M.Ş., Numerical Investigation of Fatigue Behavior of Non-Patched and Patched Aluminum/Composite Plates, *European Mechanical Science*, **2021**, 5(4):168-176
- Taguchi, G., and Konishi, S., Taguchi Methods, Orthogonal Arrays and Linear Graphs, Tools for Quality American Supplier institute, **1987**: 8-35
- Osarenmwinda, J.O., Olodu, D.D., Optimization of Injection Moulding Process Parameters in the Moulding of High Density Polyethylene (HDPE), *Journal of*

- Applied Science and Environmental Management, **2018**, 22(2): 203-206
14. Srinivas, A., Venkatesh, Y.D., Application of Taguchi Method for Optimization of Process Parameters in Improving the Surface Roughness of Lathe Facing Operation, International Refereed Journal of Engineering and Science (IRJES), **2012**, 1(3):13-19
  15. Olodu, D.D., Optimization and Analysis of Cutting Tool Geometrical Parameters using Taguchi Method, Journal of Applied Science and Environmental Management, **2018**, 22 (3): 346-349
  16. Rao, R.S., Ganesh K, C., Shetty Prakasham, R., Phil J.H., The Taguchi Methodology as a Statistical Tool for Biotechnological Applications: A Critical Appraisal, Biotechnology Journal, **2019**, 3 (4): 510–523
  17. Foster, W.T., Basic Taguchi Design of Experiments. National Association of Industrial Technology Conference, Pittsburgh, PA, **2000**
  18. Altan, M., Reducing Shrinkage in Injection Moldings through the Taguchi, ANOVA and Neural Network Methods, Journal of Material Design, **2010**, 31, 599–604
  19. Vaatainen, O, Pentti, J., Effect of Processing Parameters on the Quality of Injection Moulded Parts by Using the Taguchi Parameter Design Method, Journal of Plastic Rubber Composite, **2016**, 1: 21-217
  20. Olodu D. D., Modelling and Validation of the Production Parameters of Unalloyed Aluminium Sheets, Gazi University Journal of Science Part A: Engineering and Innovation, **2021**, 8(1): 94-108
  21. Kok, M., Production and Mechanical Properties of Al<sub>2</sub>O<sub>3</sub> Particle-Reinforced 2024 Aluminium Alloy Composites, Materials Processing Technology Journal, **2005**, 161(3): 381-387
  22. Kumar, A., Lal, S., & Kumar, S., Fabrication and Characterization of A359/Al<sub>2</sub>O<sub>3</sub> Metal Matrix Composite using Electromagnetic Stir Casting Method, Journal of Materials Research and Technology, **2013**, 2(3): 250-254
  23. Venkatesh, B., & Harish, B., Mechanical Properties of Metal Matrix Composites (Al/SiCp) Particles Produced by Powder Metallurgy, International Journal of Engineering Research and General Science. **2015**, 3(1): 1277-1284
  24. Nieh, T. G., & Chellman, D. J., Modulus Measurements in Discontinuous Reinforced Aluminum Composites, Scripta Metallurgica, **1984**, 18: 925-938
  25. Friend, C.M., The Effect of Matrix Properties on Reinforcement is Short Al<sub>2</sub>O<sub>3</sub> Fiber-Al MMCs, Journal of Materials Science, **1987**, 22(8): 3005-3010
  26. Yao, B., Hofmeister, C., Patterson, T., Sohn, Y., van den Bergh, M., Delahanty, T., & Cho, K., Microstructural Features Influencing the Strength of Trimodal Aluminum Metal-matrix-Composites, Composites Part A: Applied Science and Manufacturing, **2010**, 41(8): 933-941
  27. Saravanan, C., Subramanian, K., Ananda Krishnan, V., & Sankara N.R., Effect of Particulate Reinforced Aluminium Metal Matrix Composite, Mechanics and Mechanical Engineering, **2015**, 19(1): 23-30
  28. Prabu, S. B., Karunamoorthy, L., Kathiresan, S., & Mohan, B., Influence of Stirring Speed and Stirring Time on Distribution of Particles in Cast Metal Matrix Composite, Journal of Materials Processing Technology, **2006**, 171(2): 268-73
  29. Joardar, H., Sutradhar, G., & Das, N. S., FEM Simulation and Experimental Validation of Cold Forging Behavior of LM6 Base Metal Matrix Composites, Journal of Minerals and Materials Characterization and Engineering, **2012**, 11(10): 989-994
  30. Romanova, V. A., Balokhonov, R. R., & Schmauder, S., The Influence of the Reinforcing Particle Shape and Interface Strength on the Fracture Behavior of a Metal Matrix Composite, Acta Materialia, **2009**, 57(1): 97-107
  31. Domnita, F., and Cristian, C., Application of Taguchi Method to Selection of Optimal Lubrication and Cutting Conditions in Face Milling of AlMg<sub>3</sub>, Journal of Cleaner Production, **2011**, 19:640-645
  32. Osarenmwinda, J.O., Olodu, D.D., Effect of Barrel Temperature on the Mechanical Properties of Injection Moulded Products. Nigeria Journal of Technology (NIJOTECH), **2015**, 34(2): 292-296
  33. Adin, M., Ş., and İşcan, B., Optimization of Process Parameters of Medium Carbon Steel Joints Joined by MIG Welding using Taguchi Method. European Mechanical Science, **2022**, 6(1): 17-26
  34. Yildiz, R. A., Evaluation of Fracture Toughness and Charpy V-notch Test Correlations for Selected Al alloys. European Mechanical Science, **2022**, 6(1): 1-8